Agrin elicits membrane lipid condensation at sites of acetylcholine receptor clusters in C2C12 myotubes

Françoise Stetzkowski-Marden,* Katharina Gaus,[1,†] Michel Recouvreur,* Annie Cartaud,* and Jean Cartaud[2,*]

Biologie Cellulaire des Membranes,* Institut Jacques Monod, Unité Mixte de Recherche 7592, Centre National de la Recherche Scientifique, Université Paris 6, Université Paris 7, F-75251 Paris Cedex 05, France; and Max Planck Institute for Cell Biology and Genetics,† Dresden D-01307, Germany

Abstract The formation of the neuromuscular junction is characterized by the progressive accumulation of nicotinic acetylcholine receptors (AChRs) in the postsynaptic membrane facing the nerve terminal, induced predominantly through the agrin/muscle-specific kinase (MuSK) signaling cascade. However, the cellular mechanisms linking MuSK activation to AChR clustering are still poorly understood. Here, we investigate whether lipid rafts are involved in agrin-elicited AChR clustering in a mouse C2C12 cell line. We observed that in C2C12 myotubes, both AChR clustering and cluster stability were dependent on cholesterol, because depletion by methyl-β-cyclodextrin inhibited cluster formation or dispersed established clusters. Importantly, AChR clusters resided in ordered membrane domains, a biophysical property of rafts, as probed by Laurdan two-photon fluorescence microscopy. We isolated detergent-resistant membranes (DRMs) by three different biochemical procedures, all of which generate membranes with similar cholesterol/GM1 ganglioside contents, and these were enriched in several postsynaptic components, notably AChR, syntrophin, and raft markers flotillin-2 and caveolin-3. Agrin did not recruit AChRs into DRMs, suggesting that they are present in rafts independently of agrin activation. Consequently, in C2C12 myotubes, agrin likely triggers AChR clustering or maintains clusters through the coalescence of lipid rafts. These data led us to propose a model in which lipid rafts play a pivotal role in the assembly of the postsynaptic membrane at the neuromuscular junction upon agrin signaling.—Stetzkowski-Marden, F., K. Gaus, M. Recouvreur, A. Cartaud, and J. Cartaud. **Agrin elicits membrane lipid condensation at sites of acetylcholine receptor clusters in C2C12 myotubes.** ***J. Lipid Res.*** **2006.** 47: **2121–2133.**

Supplementary key words lipid rafts • nicotinic acetylcholine receptor • neuromuscular junction

During synapse differentiation at the neuromuscular junction, motor innervation recruits nicotinic acetylcholine receptors (AChRs) to the sites of nerve-muscle contact. AChR clustering is stimulated by the neuronally released, extracellular matrix-associated heparan sulfate proteoglycan agrin (for reviews, see 1–3). The activity of agrin in AChR clustering is mediated by a signaling machinery that includes the agrin receptor MuSK [for muscle-specific kinase receptor (4)], the AChR-associated peripheral protein rapsyn (reviewed in 2), and several intracellular enzymes (reviewed in 5). However, the mechanisms linking MuSK activation to AChR clustering at the cell surface are still poorly understood. Once activated, MuSK recruits several effectors that are known to reorganize the actin cytoskeleton (reviewed in 5). Yet, interaction of AChRs with the actin membrane cytoskeleton provides both aggregation and restricted diffusion within the lipid bilayer (6–9). However, other mechanisms could also provide AChR segregation, such as partitioning within specific lipid domains.

Cholesterol-sphingolipid-enriched lipid rafts form dynamic liquid-ordered microdomains that float freely within the fluid, liquid-disordered cellular membranes. By the nature of their structure, these domains selectively incorporate or exclude proteins; therefore, they have been proposed to function as membrane platforms for the assembly of signaling complexes and for membrane sorting (10). Because of their highly dynamic structure, these submicroscopic assemblies are able to coalesce upon clustering of their components in physiological conditions by protein-driven interactions involving, for example, caveolins (11) or reorganization of the actin cytoskeleton (12, 13) and artificially by cross-linking with antibodies or cholera toxin B subunit (CTX), a specific ligand of GM1 ganglioside (14, 15). For AChR aggregation, raft clustering might be required to generate synaptic clusters of neurotransmitter receptors characteristic of postsynaptic sites.

Abbreviations: AChR, nicotinic acetylcholine receptor; α-Bgtx, α-bungarotoxin; CTX, cholera toxin B subunit; DRM, detergent-resistant membrane; ESA, epidermal surface antigen; GP, global polarization; MβCD, methyl-β-cyclodextrin; MuSK, muscle-specific kinase.

[1] Present address of K. Gaus: Centre for Vascular Research, School of Medical Sciences, University of New South Wales, Sydney 2052 NSW, Australia.

[2] To whom correspondence should be addressed.
e-mail: cartaud@ijm.jussieu.fr

Manuscript received 21 April 2006 and in revised form 30 June 2006.

Published, JLR Papers in Press, July 1, 2006.
DOI 10.1194/jlr.M600182-JLR200

Insolubility in cold nonionic detergent and perturbation of cellular processes by cholesterol depletion with methyl-β-cyclodextrin (MβCD) have been used as tools to study the role of rafts in cell signaling and function, in particular in the maintenance and/or formation of central synapses (16). In the central nervous system, several postsynaptic proteins, including neuronal α7-AChR, gamma-aminobutyric acid receptor B($GABA_B$) receptor, N-methyl-D-aspartate (NMDA) and alpha-amino-3-hydroxy-5-methyl-4-isoxazolepropionic (AMPA) receptors, voltage-gated K^+ channel Kv2.1, postsynaptic density-95, and glutamate receptor-interacting protein, are partially associated with Triton X-100-resistant membranes (17–21). Lipid rafts exist abundantly in dendrites of cultured hippocampal neurons, in which postsynaptic proteins including AMPA receptors are enriched. Depletion of cholesterol/sphingolipids leads to the instability of these receptors and the gradual loss of synapses and dendritic spines (19). Similarly, in ciliary ganglion neurons and in PC12 cells, lipid rafts are necessary for the specific localization and stabilization of α7-AChR within the plasma membrane (18, 20). Interestingly, Oshikawa et al. (20) showed that the fractionation of PC12 cells resulted in the differential distribution of various AChR subunits: α7, which forms postsynaptic homopentameric AChRs, was recovered in the detergent-resistant membrane (DRM) fraction, whereas nonsynaptic α5 and β2 subunits were not. Thus, lipid rafts may be required to localize specific receptors to synaptic sites. A similar approach applied to transiently transfected COS-7 cells allowed us to demonstrate that muscle AChR and rapsyn are cotransported in the exocytic pathway from the Golgi apparatus to the cell surface within lipid rafts (22). More recently, Campagna and Fallon (23) reported that in C2C12 myotubes, CTX favors agrin-induced AChR clustering and that depletion of cholesterol disrupts AChR aggregates, supporting the notion that lipid rafts contribute to synaptic organization at the neuromuscular junction.

As cold detergent extraction may cause artifactual lipid aggregation and cholesterol depletion may not be specific to rafts (24, 25), alternative microscopic techniques, such as fluorescence resonance energy transfer (FRET), Laurdan two-photon microscopy, and single-particle tracking, as well as detergent-free purification procedures have been developed to study raft properties. Here, we combine a number of these approaches to study the agrin-induced AChR clusters of C2C12 myotube plasma membrane. We use immunofluorescence to quantify AChR clustering and the fluorescent lipid dye Laurdan in conjunction with two-photon laser scanning microscopy for the biophysical characterization of AChR clusters. Laurdan's fluorescence emission spectrum depends on the fluidity of its membrane environment (26), and this approach was used to verify the cholesterol dependence of AChR clustering. Furthermore, we analyzed DRMs from C2C12 myotubes and compared them with two alternative detergent-free extraction procedures. The biochemical data showed that AChR fractionated within light cholesterol-enriched DRMs independently of agrin treatment. Together, these data indicate that in muscle fibers, lipid raft coalescence may serve as a signaling platform to concentrate AChRs at synaptic sites after agrin/MuSK activation.

MATERIALS AND METHODS

Antibodies and reagents

Mouse monoclonal anti-syntrophin [1351E (27)] and anti-rapsyn [1234 (28)] antibodies were provided by Prof. S. Froehner (University of Washington, Seattle, WA) or purchased from Abcam, UK. Monoclonal anti-transferrin receptor (H 68.4) was a gift from Prof. J. M. Trowbridge (San Diego, CA). Monoclonal anti-AChR α-subunit (clone 26), anti-flotillin-2/epidermal surface antigen (ESA), and anti-caveolin-3 antibodies were obtained from Transduction Laboratories (Lexington, KY). CTX, anti-CTX, anti-α-tubulin, MβCD, and Triton X-100 were purchased from Sigma (St. Louis, MO). The following reagents and antibodies were used for immunofluorescence: FITC and Alexa 555-conjugated α-bungarotoxin (α-Bgtx) and Laurdan (6-dodecanoyl-2-dimethylaminonaphthalene) were from Molecular Probes, Inc. (Eugene, OR), and rhodamine isothiocyanate-conjugated secondary antibodies were from Jackson Immunoresearch (West Grove, PA).

Cell cultures

The culture of C2C12 cell line (adult C3H mouse leg muscle; catalog No. CRL-1772; American Type Culture Collection, Manassas, VA) was initiated with 10% fetal bovine serum in DMEM (Gibco, Eggenheim, Germany) complemented with 100 U/ml penicillin and streptomycin and 0.5% (v/v) glutamine for 3–4 days. Myotube differentiation was achieved in 3% horse serum in DMEM supplemented with 100 U/ml penicillin and streptomycin and 0.5% (v/v) glutamine for 5–7 days. AChR clustering was elicited by overnight incubation with 5 ng/ml recombinant 90 kDa C-terminal rat agrin (C-Ag $_{3,4,8}$) purchased from R&D Systems (Minneapolis, MN). For immunofluorescence studies, cells were plated on glass coverslips covered with a thin layer of Matrigel® (Becton Dickinson, Bedford, MA) onto a six-well plate. For biochemical studies, cells were grown in 75 cm^2 flasks. All cell cultures were maintained at 37°C in a humidified air atmosphere containing 5% CO_2.

Drug treatments

The depletion of cholesterol from C2C12 myotube membranes was performed by incubation of cultures with MβCD (10 mM) for 30 min at 37°C (14, 18). After washing, the cells were processed either for AChR and Laurdan labeling or for AChR quantification as indicated (see below).

Preparation of DRM fractions from C2C12 myotubes

Three different methods were used to purify DRM fractions from differentiated myotubes: the traditional nonionic detergent (Triton X-100) at 4°C (29), detergent-free at pH 11 (30), or shearing in an isotonic buffer containing Ca^{2+}/Mg^{2+} (31).

For Triton X-100, fully differentiated C2C12 myotubes were washed in PBS and buffer A (25 mM *N*-morpholino-ethane-sulfonic acid, pH 7.4, 150 mM NaCl, and 2 mM EDTA). The cells were then suspended in ice-cold 1% Triton X-100 (protein-detergent ratio of ≥1:1, w/w) in 2 ml of buffer A supplemented with a protease inhibitor cocktail (1 μg/ml leupeptin, 1 μg/ml pepstatin, 1 mM benzamidine, 3 μg/ml aprotinin, and 2.5 μM phenylmethylsulfonyl fluoride), homogenized with 12–15 strokes of a Dounce homogenizer, and incubated for 1 h on ice.

For alkaline extraction C2C12 myotubes were homogenized in 0.5 M sodium carbonate, pH 11 (30). After sodium carbonate extraction, cells were sonicated three times for 2 min on ice in a bath sonicator.

For both extraction protocols, an equal volume of 80% (w/v) sucrose in buffer A was added to the cell lysates (2 ml) and placed in the bottom of an ultracentrifugation tube. Cell lysates were overlaid successively with 4 ml of 30% sucrose and 4 ml of 5% sucrose in buffer A (supplemented with 250 mM sodium carbonate for the detergent-free extraction protocol). After centrifugation at 39,000 rpm in a Beckman SW41 Ti rotor for 18 h at 4°C, 1 ml fractions were collected from top to bottom (designated 1–12).

A third simplified method adapted from Macdonald and Pike (31) was used: myotubes were washed in buffer P (20 mM Tris, pH 7.8, 1 mM $CaCl_2$, and 1 mM $MgCl_2$) containing 250 mM sucrose and homogenized with 20 strokes of a Dounce homogenizer. Cells were then lysed in buffer P supplemented with antiproteases by five passages through an 18 gauge, 1.5 inch needle followed by 15 passages through a 21 gauge, 2 inch needle. Lysates were centrifuged at 1,000 *g* for 10 min. The resulting postnuclear supernatants were collected and saved. The pellet was again lysed and centrifuged. Both supernatants were combined and mixed with an equal volume of 80% (w/v) sucrose in buffer P and placed in the bottom of an ultracentrifugation tube. Cell lysates were overlaid successively with 2 ml of 35%, 2 ml of 30%, 2 ml of 20%, and 2 ml of 5% sucrose in buffer P free of sucrose, and gradients were centrifuged at 39,000 rpm in a Beckman SW41 Ti rotor for 18 h at 4°C.

Western blot and dot blot analyses

Proteins from gradient fractions were precipitated with 10% trichloracetic acid, washed with 80% cold acetone, dissolved in Laemmli buffer (32), separated on 10% SDS-PAGE (Mini Protean II; Bio-Rad, Richmond CA), and electrotransferred onto nitrocellulose paper (Schleicher and Schuell, Dassel, Germany). Western blots were probed using various primary antibodies: anti-AChR α-subunit (1:300), anti-rapsyn (1:400), anti-caveolin-3 (1:15,000), anti-flotillin-2/ESA (1:7,500), anti-syntrophin (1:10,000), anti-transferrin receptor (1:3,000), and anti-α-tubulin (1: 30,000) as well as appropriate HRP-conjugated secondary antibodies with ECL detection (Amersham Pharmacia Biotech) and exposure to Fuji X-ray films. To reveal the distribution of GM1 in the gradients, 50 μl of each fraction before TCA precipitation was spotted onto nitrocellulose membranes using a Bio-Rad Dot Blot apparatus. GM1 was detected with CTX and anti-CTX antibodies, followed by ECL detection.

Immunofluorescence microscopy

C2C12 myotubes were rinsed with PBS and fixed at 4°C for 15 min with 3% paraformaldehyde in 0.1 M phosphate buffer, pH 7.4. Fixed cells were rinsed with PBS, and where needed (for immunodetection of flotillin-2 or caveolin-3), permeabilized with 0.1% Triton X-100 in PBS for 5 min at room temperature (or with 95% methanol for 5 min at −20°C) and washed. After preincubation for 30 min at room temperature in PBS containing 1% BSA and 5% goat serum, C2C12 myotubes were incubated for 1 h at room temperature with the primary antibodies anti-caveolin-3 (1:400) or anti-flotillin-2/ESA (1:100) in PBS supplemented with 0.1% BSA and 0.5% goat serum, then rinsed three times with PBS for 5 min and incubated with the secondary antibody (rhodamine isothiocyanate-conjugated goat anti-mouse; 1:400) for 30 min at room temperature. In all experiments, AChR detection was achieved by FITC-conjugated α-Bgtx (3 μg/ml). Before observation, samples were mounted in Citifluor (UKC Chemlab). Micrographs were taken with a Leica DMR microscope (Leica Systems) equipped with PL Fluotar ×40 or Plan Apo ×63 oil-immersion optics and a Micro Max cooled charge-coupled device camera (Princeton Instruments, Inc.) operating at full resolution. Digital images were recorded using the Meta View Imaging System (Universal Imaging Corp.) and prepared for publication using Adobe Photoshop.

Laurdan two-photon microscopy

Differentiated C2C12 myotubes were labeled with Laurdan by incubating washed cells (1% horse serum in DMEM) with 5 μM Laurdan in 1% horse serum in DMEM for 30 min at 18°C or 37°C. Myotubes were washed in PBS and fixed with 3% paraformaldehyde in 0.1 M phosphate buffer, pH 7.4. After washing, cells were labeled with Alexa 555-conjugated α-Bgtx (3 μg/ml; Molecular Probes), washed, and mounted in Citifluor. Multiple-photon excitation of Laurdan fluorescence was at 800 nm with a Verdi/Mira 900 laser system, and intensity images were recorded simultaneously in the range of 400–450 nm and 450–530 nm with a Bio-Rad microscope. The relative sensitivity of the two channels was calibrated with 5 μM Laurdan in DMSO for each experiment. For confocal microscopy, a helium-neon laser was used to excite Alexa 555 with appropriate cutoff filters and pinhole widths. For all images, a 100× oil objective, numerical aperture 1.4, was used. Alexa immunofluorescence stain was imaged first and then Laurdan at the same focal depth. For Laurdan image analysis, all calculations were carried out in floating point format and images converted into eight bit unsigned images for presentation using the imaging software WIT. The global polarization (GP), defined as:

$$GP = \frac{I_{(400-450)} - I_{(450-530)}}{I_{(400-450)} + I_{(450-530)}}$$

was calculated for each pixel using the two Laurdan intensity images. GP images were pseudocolored in Adobe Photoshop. To determine GP values at α-Bgtx clusters, confocal images were used to mask the GP images; the confocal images defined the regions of interest, and the mean GP values of the regions of interest were determined for each image. GP values were corrected using the G-factor obtained for Laurdan in DMSO for each experiment (33).

Image quantification

To determine the line profiles of the AChR clusters, a line was drawn along the main axis of myotubes and the fluorescence intensity was plotted versus relative distance using NIH ImageJ software 1.26t (Bethesda, MD). To estimate the magnitude of the effect of drug treatments on AChR clusters, the number and average size of clusters were measured using a calibrated mesh. The average length of AChR aggregates (l) was estimated according to

$$l = \pi nd/4N$$

where n is the number of intersections between clusters and the mesh, d is the size of the mesh, and N is the total number of clusters. For each experiment, five optical fields selected at random were analyzed at a magnification of 1,600×.

Quantification of proteins and cholesterol

The total amount of proteins in the C2C12 cells as well in the various fractions collected from the gradients was determined according to the Pierce protocol of the BCA™ Protein Assay Reagent Kit (Rockford, IL). Cholesterol quantification was based

upon the cholesterol oxidase method for cholesterol determination by spectrophotometry using the Thermo Trace assay (Thermo Electron Corp., Melbourne, Australia). Calibration was done with aqueous standard solutions of cholesterol (Thermo Electron Corp.). For total cholesterol determination in C2C12 myotubes, cells were previously washed in lipid-free synthetic culture medium (DMEM) and lysed with Triton X-100.

Quantification of AChR in C2C12 myotubes

Quantification of AChR (34, 35) expressed at the cell surface was determined by incubating fixed (3% paraformaldehyde, 10 min at 4°C), differentiated C2C12 myotubes with ^{125}I-α-Bgtx. For intracellular AChR quantification, fixed C2C12 myotubes were incubated with cold α-Bgtx (5 nM) for 1 h at 4°C to block the α-Bgtx binding sites of the cell surface, then permeabilized with 0.1% Triton X-100 for 5 min. Total AchR (surface plus intracellular) was quantified on cells also permeabilized with 0.1% Triton X-100. For cell surface, intracellular, and total AChR quantification, cells were incubated for 2 h on ice with 5 nM ^{125}I-α-Bgtx (150 Ci/mmol; Amersham Biosciences) in PBS containing 1 mg/ml BSA, followed by three washings on ice with PBS/BSA. Cells were lysed in PBS containing 1% SDS at 37°C for 1 h. Cells lysates were collected, and ^{125}I radioactivity was counted for 1 min on a MR480 γ counter (Kontron Electronik, Eching, Germany). Nonspecific binding determined after competition of ^{125}I-α-Bgtx binding with a large excess of cold α-Bgtx (5 μM) was generally <5–10%. Each experiment was done in triplicate. In all experimental conditions, we verified that the same amount of total protein was present and expressed the data as percentage of total AChR in control myotubes.

Negative staining electron microscopy

Samples of DRM fractions taken directly from the gradients were supplemented with 10 μg/ml bacitracin (Sigma). Ten microliter drops were then deposited onto carbon-coated electron microscopy grids. Negative staining was achieved by washing the grids with 100 μl of 1% (w/v) uranyl acetate in water and dried with filter paper. Grids were observed in a Philips (Eindhoven, The Netherlands) EM12 electron microscope fitted with a LaB6 filament and operation at 80 keV. Micrographs were taken on Kodak electron microscope film.

RESULTS

Cholesterol is required for AChR clustering in C2C12 myotubes

As lipid rafts are enriched in cholesterol, the removal of cholesterol from cell membranes causes the dispersion of lipid rafts within the fluid phase of the cell membrane and perturbs signaling efficiency (14, 18, 36). To determine whether cholesterol-enriched lipid domains are involved in AChR clustering, we used MβCD, a useful tool that has been shown to extract cholesterol from biological membranes with high preference over other lipid species, to selectively deplete cholesterol from the cell membrane in C2C12 myotubes. Similar to what is reported with other cells, MβCD treatment (10 mM, 30 min) of C2C12 myotubes released ~60% of total cellular cholesterol. We thus addressed whether MβCD treatment perturbs already established AChR aggregates, which were previously induced by agrin at the surface of myotubes. In myotubes incubated overnight with agrin, numerous AChR clusters measuring up to 10–20 μm (mean length, 4.0 ± 1.0 μm) were detected at the surface of myotubes by fluorescence microscopy using FITC-conjugated α-Bgtx as a marker for AChRs (**Fig. 1A**). In cholesterol-depleted cells, small dispersed AChR aggregates with a mean size of 1.3 ± 0.2 μm were observed instead of the large AChR clusters (Fig. 1B). Plots of line profiles along the main axis of myotubes showing the fluorescence intensity versus distance illustrated the dispersion of AChR clusters into smaller patches after MβCD treatment (Fig. 1C, D, corresponding to Fig. 1A, B, respectively), which does not result in a larger number of smaller clusters. For control cultures, we found 47 ± 8 clusters/field (n = 5) and 58 ± 10 clusters/field (n = 3) after MβCD treatment. In a second series of experiments, we asked whether the presence of cholesterol is required for agrin-induced AChR clustering. We thus depleted cholesterol from myotubes using MβCD before induction of AChR clustering by agrin. In these conditions, no large AChR clusters (⩾4 μm) were observed (Fig. 1E, F, control). Cholesterol-depleted myotubes were thus no longer able to form typical AChR clusters, as recently reported by Campagna and Fallon (23).

In previous works by us and others (22, 37, 38), lipid rafts have been shown to be required for intracellular trafficking and surface transport of AChRs. To ascertain the role of lipid rafts on agrin-elicited AChR clustering, rather than the effect of the depletion of cholesterol on AChR biosynthesis and/or surface expression, we quantified surface, intracellular, and total AChRs in control and MβCD-treated myotubes by means of ^{125}I-α-Bgtx binding. We observed that MβCD-treated myotubes exhibit similar total [93 ± 13% vs. 100 ± 19% (n = 6) for MβCD-treated myotubes and controls, respectively], cell surface [49 ± 14% vs. 53 ± 14% (n = 3)], and intracellular [47 ± 21% vs. 60 ± 15% (n = 3)] AChR content compared with controls (all data are expressed as percentage of total AChR in control myotubes = 100%). These data show that in our experimental conditions (10 mM MβCD, 30 min), cholesterol depletion of myotubes has no major effect on AChR biosynthesis, surface transport, or internalization. We thus conclude that cholesterol is required for the agrin-elicited AChR clustering.

AChR clusters correspond to condensed membrane domains of the myotube surface

So far, our data in agreement with other reports (23) suggest a role of cholesterol in AChR clustering. Lipid rafts, as an entity, constitute a highly ordered membrane domain that is distinct from the more fluid surroundings. To demonstrate that AChR-rich microdomains indeed correspond to ordered domains, we applied Laurdan two-photon fluorescence microscopy, which allows the direct visualization of membrane order (26). To assess the degree of lipid condensation at AChR clusters, C2C12 myotubes were labeled with Laurdan before or after agrin induction and imaged, and the intensity images were converted into GP images as reported previously (33, 39). Regions of high GP values (0.25 to 0.55) corresponded to ordered domains

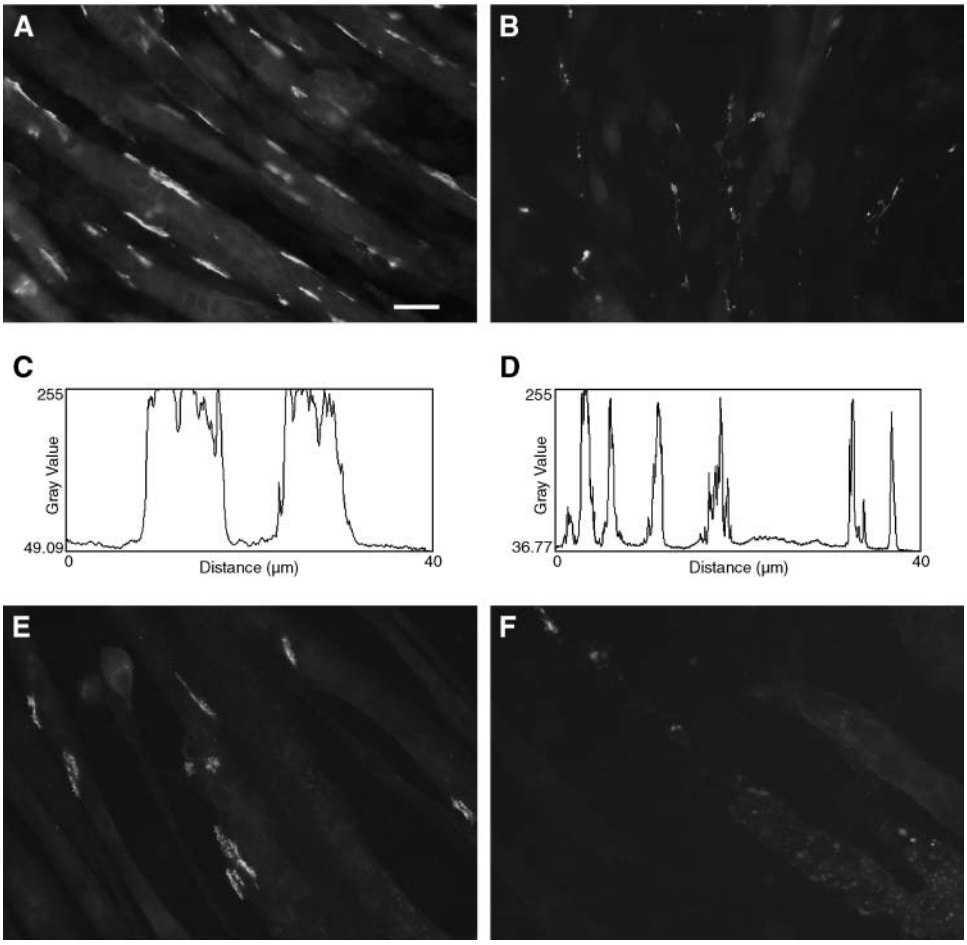

Fig. 1. Cholesterol is required to induce and maintain nicotinic acetylcholine receptor (AChR) clusters in C2C12 myotubes. A, E: Agrin-elicited AChR clusters were detected by FITC-conjugated α-bungarotoxin (α-Bgtx) labeling in C2C12 myotubes. B: Cholesterol depletion by methyl-β-cyclodextrin (MβCD) after agrin (10 mM, 30 min at 37°C; see Materials and Methods) induced the dispersion of agrin-induced AChR clusters into patches of smaller size. C, D: Fluorescence intensity for AChR aggregates was plotted versus relative distances along the main axis of myotubes corresponding to A, B, respectively. F: Depletion of cholesterol before agrin treatment prevented the formation of AChR aggregates at the surface of myotubes. Internal controls (A, F) were provided for each set of experiments. Bar = 10 μm.

(colored yellow to red), whereas low GP (−0.05 to 0.25) corresponded to fluid domains (colored green). **Figure 2** shows control (A–C) and agrin-treated (D–F) myotubes labeled with Laurdan and α-Bgtx. In control cells (A, C), no regions of high GP were detected (mean GP = 0.234 ± 0.028; n = 24) (**Table 1**). In agrin-treated myotubes (D, F), GP values of α-Bgtx-labeled AChR clusters were increased significantly (mean 0.303 ± 0.088; n = 38, $P < 0.001$), with peak values reaching 0.6–0.8 (see line plot in F). The line plot (F) shows the profile of GP values and α-Bgtx fluorescence intensities across three AChR clusters (E), indicating that high GP regions were associated with most AChR clusters (open arrows). However, some AChR clusters did not correspond to particular condensed membrane domains (closed arrow in Fig. 2F). Labeling myotubes at 18°C to block endocytosis (Table 1) yielded the same results, with mean GP values of agrin-induced AChR clusters of 0.312 ± 0.065, indicating that AChR clusters reside in ordered membrane domains at the cell surface. Furthermore, cholesterol depletion with MβCD (10 mM, 30 min) before or after agrin treatment (G–I) significantly decreased the mean GP value of toxin-stained membranes (J–L) compared with control, agrin-treated myotubes (Table 1). Importantly, MβCD treatment did not globally reduce membrane structure below control membranes (compare average GP values in I and L with that in C), suggesting that MβCD treatment was specific to cholesterol-enriched domains. We conclude that agrin-induced AChR clusters resemble lipid rafts biophysically and that the formation, size, and structure of membrane domains after agrin signaling are dependent on cholesterol.

AChR partitions within DRMs in C2C12 cells

The biochemical characterization of lipid rafts from various cell types has been mainly facilitated by isolation procedures based on their relative insolubility in cold, nonionic detergents (typically 1% Triton X-100). However, it has become clear that detergent treatment itself

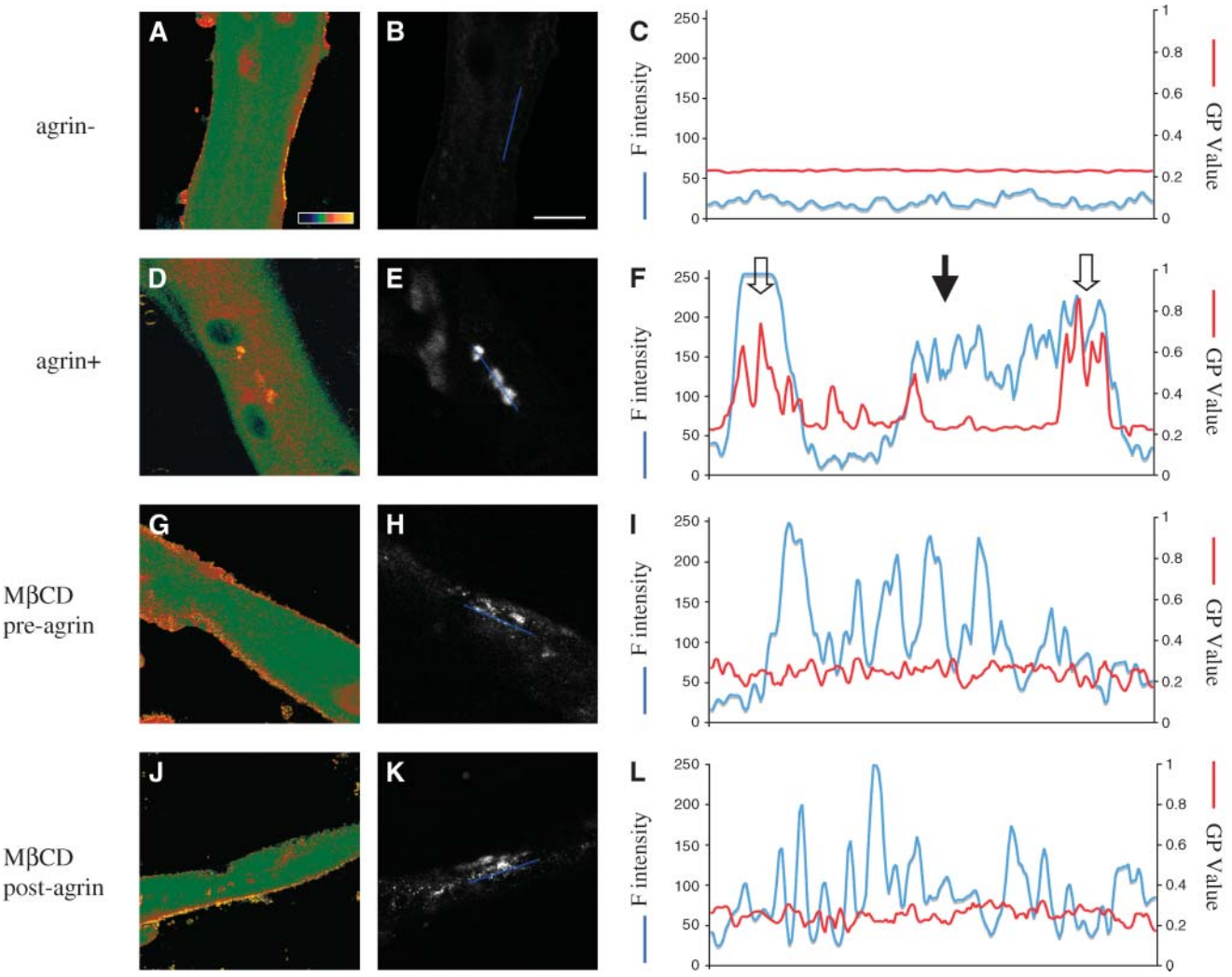

Fig. 2. Membrane condensation at agrin-induced AChR clusters in C2C12 myotubes. Laurdan-labeled C2C12 myotubes were simultaneously imaged for Laurdan intensity in two channels (400–450 nm and 450–530 nm) using two-photon laser scanning microscopy and for Alexa 555-conjugated α-Bgtx. Intensity images were converted to global polarization (GP) images as described in Materials and Methods. A, D, G, J: GP images were pseudocolored for low and high GP from blue to yellow, respectively (scale in A). B, bar = 10 μm. B, E, H, K: Confocal images of Alexa 555-α-Bgtx staining of AChRs of the same fields and focal depth as the corresponding GP images. C, F, I, L: Plot profiles of the fluorescence (F) intensity of the toxin (blue, left *y* axis) and the GP values (red, right GP axis) along the blue lines indicated in B, E, H, K, respectively. A–C: Control myotubes. D–F: Agrin-treated myotubes. G–I: MβCD before agrin. J–L: MβCD after agrin. The plot profile in F disclosed high GP corresponding to two AChR clusters (open arrows) and an AChR cluster with low GP (closed arrow). Note that GP values of MβCD-treated myotubes declined to control values (compare red plots in I and L with that in C).

TABLE 1. GP values at nicotinic acetylcholine receptor cluster membranes in agrin-treated and cholesterol-depleted C2C12 myotubes

Treatment	Mean GP Value of Receptor Clusters
No agrin	0.234 ± 0.028 (n = 24)[a,b]
Agrin	0.303 ± 0.088 (n = 38)[a,c,d]
Agrin with Laurdan labeling at 18°C	0.312 ± 0.065 (n = 15)[b]
MβCD after agrin	0.255 ± 0.071 (n = 20)[c]
MβCD before agrin	0.262 ± 0.058 (n = 21)[d]

GP, global polarization; MβCD, methyl-β-cyclodextrin. Values shown are means ± SD. All experiments were carried out at 37°C, except as indicated.

[a] $P < 0.001$.
[b] $P < 0.001$.
[c] $P < 0.05$.
[d] $P < 0.05$.

can induce the formation of lipid domains, which do not exist in the native membranes before detergent extraction. To circumvent a possible artifactual association of AChR with DRMs, alternative detergent-free extraction procedures have been developed (30, 31). Here, we used three different extraction protocols to characterize synaptic components in DRM fractions purified from cultured muscle cells. In a first approach, we applied the standard Triton X-100 extraction protocol on C2C12 myotubes to isolate DRMs in a 5:30:40% discontinuous sucrose density flotation gradient. Fractions were analyzed for total protein and lipid rafts (cholesterol and GM1 ganglioside; **Fig. 3A**). Relatively little protein was present in the light/DRM fractions (fractions 4–6, corresponding to the 5/30% interface), the bulk of the proteins being found in

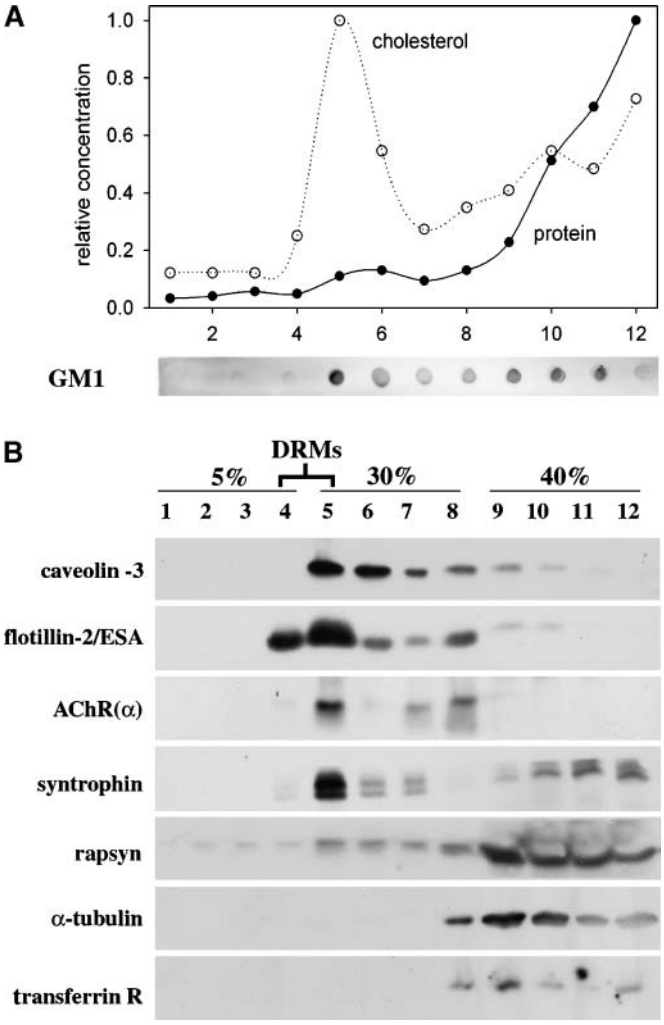

Fig. 3. Detergent-resistant membrane (DRM) association of AChR, syntrophin, and rapsyn in nonionic detergent extracts of C2C12 myotubes. A: Distributions of cholesterol, proteins, and GM1 across the sucrose step gradient. Protein and cholesterol contents of each fraction were determined as indicated in Materials and Methods and normalized to 1, according to their respective maximal values. For GM1 distribution along the gradient, dot blots were made using cholera toxin B subunit (CTX) and anti-CTX antibodies followed by ECL detection. B: Western blots showing the distribution of caveolin-3, flotillin-2/epidermal surface antigen (ESA), AChR (α-subunit), syntrophin, rapsyn, transferrin receptor (transferrin R), and tubulin along the sucrose density gradients after extraction of myotubes on ice with Triton X-100 (1:1 Triton X-100-protein ratio, w/w). AChR and syntrophin comigrated with the two raft markers in light fractions 4–6 (5/30% interface), well separated from nonraft transferrin receptor and tubulin recovered in the heavy fractions 9–12 at the bottom of the gradient. Small amounts of rapsyn were also recovered in the DRM fractions.

the dense fractions, as generally reported. Conversely, cholesterol and GM1 levels were high in the DRM fractions (~150 μg cholesterol/mg protein) compared with high-density fractions (10–20 μg cholesterol/mg protein). These properties are typical characteristics of rafts/DRMs. We further characterized these fractions by immunoblotting using antibodies against known raft proteins such as caveolin-3, the muscle isoform of caveolin (40), and flotillin-2/ESA, the flotillin isoform upregulated during the differentiation of skeletal myoblasts (41). As shown in Fig. 3B, these two markers are enriched in fractions 4–6, as expected for DRMs. Furthermore, light fractions, which displayed canonical biochemical properties of lipid rafts, also contained robust amounts of AChR. Interestingly, the signaling/adaptor protein syntrophin, a postsynaptic protein concentrated at AChR-rich sites in skeletal muscles (27, 42), was also recovered in DRM fractions. Small amounts of rapsyn were also detected in these fractions. Conversely, the nonraft proteins tubulin and transferrin receptors are present almost exclusively in the heavier fractions of the gradient. Consistent with other reports (43, 44), we also observed that the protein-detergent (Triton X-100) ratio was critical for AChR partitioning in DRMs. A minimal protein-detergent ratio of 1:1 (w/w) was required to recover AChRs within light fractions of the gradients as DRMs. These data are in agreement with a previous work carried out in transiently transfected COS-7 cells, in which we showed that the majority of AChR was recovered in Triton X-100-resistant membranes (22).

Because DRMs were isolated from postlysis membranes, which might either induce the formation of lipid domains or exclude proteins that are weakly associated with rafts, we used alternative detergent-free methods for DRM isolation: extraction of myotubes by sodium carbonate, pH 11, sonication (30) (**Fig. 4**) or a simplified extraction method using shearing of cells in a divalent cations buffer [calcium-magnesium buffer (31)] (**Fig. 5**). In alkaline-extracted myotubes, the distributions of cholesterol, GM1, and total protein along the gradients as well as the cholesterol-protein ratio of the light fractions (5/30% interface; Fig. 4) were similar to those obtained after Triton X-100 extraction (Fig. 3A). AChR was almost totally recovered in low-buoyancy fractions (Fig. 4B), together with raft markers flotillin-2 and caveolin-3. Again, part of rapsyn immunoreactivity was recovered in DRMs. Extraction in Ca^{2+}/Mg^{2+} buffer, according to Macdonald and Pike (31), resulted in the isolation of a cholesterol-rich fraction at the 30/35% interface of the sucrose gradient in which flotillin-2 and AChR were totally recovered (Fig. 5B). Compared with the two other purification procedures, a slight shift toward the light fractions was observed for GM1 ganglioside compared with cholesterol (Fig. 5A). Note that the highest intensities of AChR and flotillin immunoreactivities were more coincident with cholesterol-enriched fractions than with GM1-enriched fractions. This shift of GM1 could result from the more analytical sucrose gradient, which allows a fine separation of subclasses of DRMs with different cholesterol/GM1 ratios. Together, the biochemical analysis of DRMs obtained from three extraction procedures based on different biochemical principles demonstrated that AChR, syntrophin, rapsyn, and possibly other synaptic components such as MuSK (data not shown) are associated with raft-like membrane domains.

Electron microscopic examination of the DRM samples derived from the three extraction procedures (**Fig. 6**) disclosed vesicular profiles with diameters ranging from 0.1 to 0.5 μm. Such structures are similar to those of

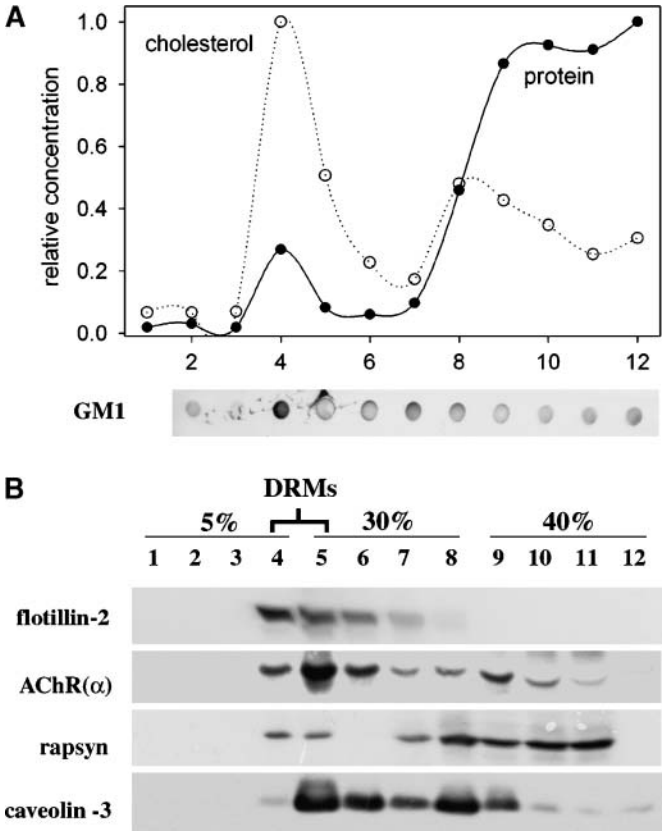

Fig. 4. Alkaline extraction of DRMs from C2C12 myotubes. A: Distributions of cholesterol, proteins, and GM1 across the sucrose step gradient after carbonate extraction of C2C12 myotubes. Cholesterol, GM1, and total protein profiles appear similar to those obtained after Triton X-100 extraction. B: AChR partitioned in the light fractions 4–6, as did flotillin-2 and caveolin-3. Rapsyn was partially recovered in the DRM fractions.

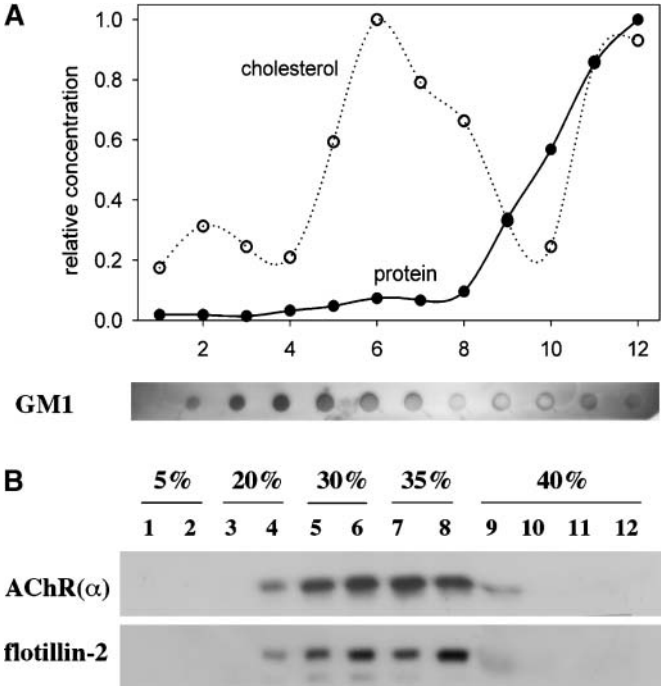

Fig. 5. Isotonic Ca^{2+}/Mg^{2+} extraction of DRMs from C2C12 myotubes. A: Distributions of cholesterol, proteins, and GM1 across an expanded sucrose step gradient after isotonic Ca^{2+}/Mg^{2+} extraction. B: Cholesterol-enriched fractions were recovered in the 30% and 35% layers together with AChR and raft marker flotillin-2. Note that in this expanded gradient, GM1 ganglioside-enriched membranes float with a slight shift toward light fractions.

postsynaptic density-70-enriched dendritic raft fraction isolated from rat forebrain (45). The Ca^{2+}/Mg^{2+} fraction was more homogenous than the two others and differed in vesicle mean diameter (0.1–0.2 μm). Given the small size attributed to native rafts in situ (46), these large DRM vesicles likely correspond to aggregates of raft domains.

To assess whether agrin recruits AChR into rafts, we analyzed the DRM fractions obtained from control and agrin-treated myotubes. In all extraction conditions (Triton X-100, pH 11, and Ca^{2+}/Mg^{2+} buffer), we were not able to detect any significant difference in the distribution patterns of AChRs along the gradients (**Fig. 7**) between control and agrin-treated myotubes. We conclude that AChRs are constitutively associated with cholesterol-rich membrane domains and that agrin did not significantly contribute to the translocation of AChR into lipid rafts.

AChRs, caveolae, and flotillin-enriched rafts segregate as distinct microdomains at the cell surface of myotubes upon agrin engagement

In mammalian cells, several classes of rafts have been described, most prominently caveolin-containing membrane invaginations (caveolae) and non-caveolin-containing rafts (47). Owing to their specific biochemical composition, all DRMs display similar buoyancy; therefore, they cannot be separated by current gradient flotation centrifugation. It is likely that all proteins enriched in the light fractions from C2C12 myotubes resulted from the accumulation of the various raft subclasses. To determine whether caveolin, flotillin, and AChR are present in specialized subclasses of rafts in situ, we studied the localizations of AChR clusters, caveolin-3, and flotillin-2 by immunofluorescence microscopy in C2C12 myotubes after agrin treatment. **Figure 8** shows that caveolin-3 (A, B) and flotillin-2 (C) were both excluded from agrin-elicited AChR clusters. A similar mutual exclusion between AChR and caveolin-1-rich membrane domains has been observed in transfected COS-7 cells (22). Thus, we conclude that upon agrin engagement, AChR-enriched rafts become clustered at the cell surface independently of caveolin-3 or flotillin-2-enriched raft subclasses. These data suggest that several functionally specialized subsets of rafts coexist at the surface of myotubes and that AChR clustering results from the regulated coalescence of one (or a few) distinct raft subclass(es) enriched in postsynaptic components.

DISCUSSION

Cholesterol- and sphingolipid-enriched microdomains or lipid rafts have been added to the bilayer model to ex-

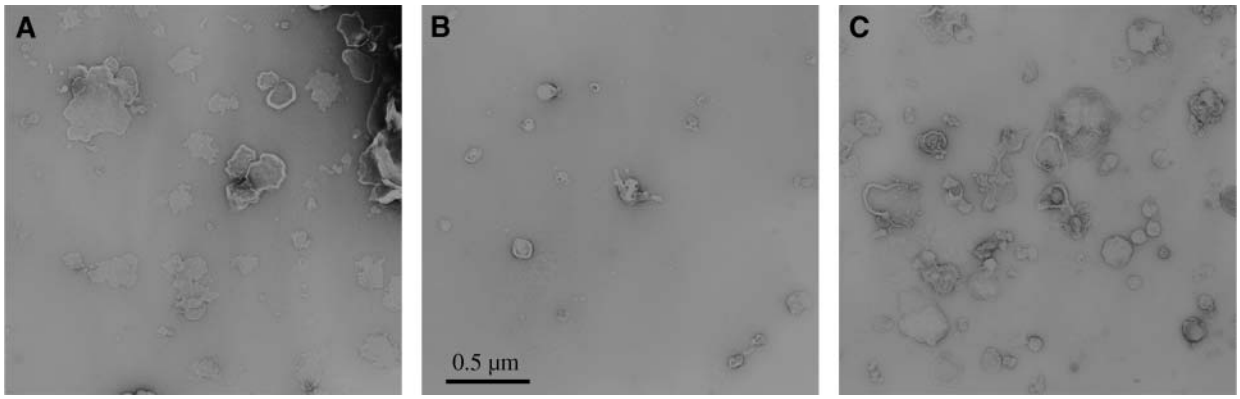

Fig. 6. Electron micrographs of DRM fractions from C2C12 myotubes. Negatively stained AChR-rich DRM fractions from the three different purification protocols are shown. A: Triton X-100. B: Isotonic cation buffer. C: pH 11.

plain lateral segregation within cellular membranes. As such, lipid rafts would regulate local concentrations of membrane proteins and lipids. Accordingly, rafts have been implicated in protein and lipid sorting and trafficking, vesicle formation and docking, entry and exit of pathogens, and receptor-mediated cell signaling (48, 49). Because lipid rafts can move laterally and cluster into larger patches (39), they have been proposed to play a role in the redistribution of specific molecules to specialized cellular structures. Indeed, rafts have been shown to favor the formation and maintenance of synaptic receptor clusters in neurons of the central nervous system (17–20) and in myogenic cells (23).

Here, we show that in C2C12 myotubes, agrin-elicited AChR clusters correlated with condensed membrane domains: the biophysical hallmark of lipid rafts. Furthermore, we demonstrate that the formation of AChR clusters and their size, as well as the structure of the membrane domains they reside in, depend on cholesterol. We also report that three different extraction procedures generated DRMs with high cholesterol/GM1 ganglioside content and that these are enriched in several postsynaptic components, notably AChR, syntrophin, and raft markers

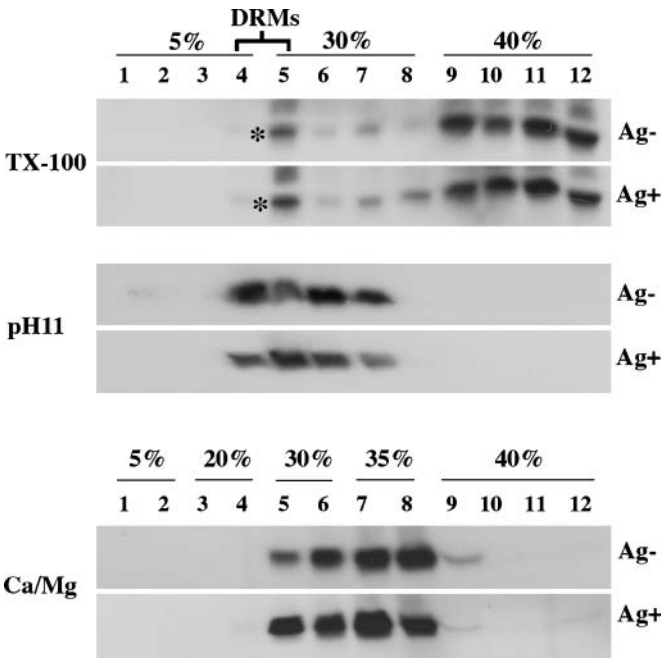

Fig. 7. Absence of any effect of agrin on DRM association of AChR. The effect of agrin on the distribution of AChR in step gradients after Triton X-100 (TX-100), pH 11, and Ca^{2+}/Mg^{2+} buffer was monitored by Western blotting. To minimize individual culture or extraction variations, control and agrin-treated myotubes were strictly processed in the same conditions. In the Triton X-100 extraction conditions, we selected an experiment in which AChR was recovered in both light and heavy fractions to optimize the detection of possible differential AChR partitioning between DRM and non-DRM. Asterisks indicate the position of the AChR α-subunit (42 kDa).

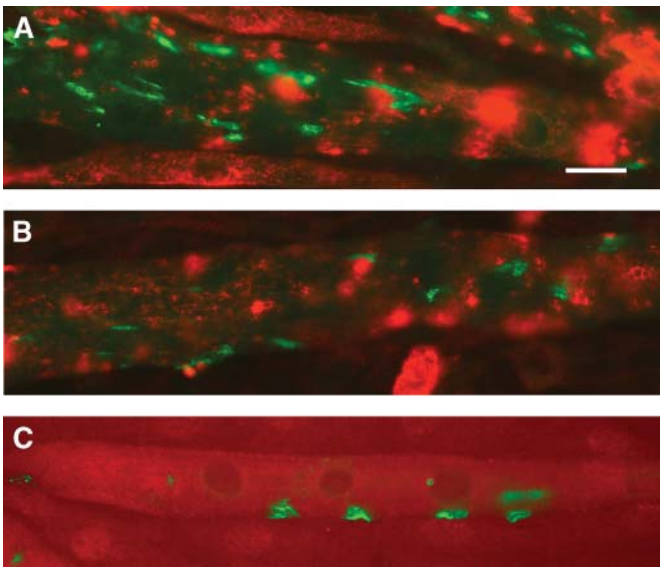

Fig. 8. AChR aggregates independently of caveolin-3 and flotillin-2/ESA-enriched microdomains in agrin-treated C2C12 myotubes. FITC-α-Bgtx labeling of AChR clusters (green fluorescence) did not coincide with anti-caveolin-3 (A, B) or anti-flotillin-2/ESA (C) labeling (red fluorescence). Merged images are shown. Bar = 10 μm.

flotillin-2 and caveolin-3. Interestingly, agrin did not recruit AChR into DRMs, suggesting that AChR is present in rafts independent of agrin activation. Together, these data suggest that lipid rafts represent platforms for AChR clustering at the neuromuscular junction.

A major goal of this study was to establish whether the condensation of membrane domains or ordered membrane phases, by definition lipid rafts, correlates with AChR aggregation in myotubes upon agrin engagement. Laurdan fluorescence microscopy has been instrumental in quantifying formation membrane order and defining the cellular requirements of condensed membrane domains (26). By visualizing lipid structure and raft domains in living cells, Laurdan two-photon microscopy provided strong support for the lipid raft hypothesis. Generally, live or fixed cells displayed two distinct plasma membrane regions. Those with a mean GP of 0.10–0.25 correspond to liquid-disordered phases, and regions with a mean GP of 0.35–0.55 correspond to liquid-ordered phases (33, 39, 50). Our experiments reveal that AChR clusters in agrin-treated myotubes are associated with mean GP values (0.303 ± 0.088 at 37°C and 0.312 ± 0.065 at 18°C) statistically higher than that of the membranes of untreated myotubes (0.234 ± 0.028). Some discrete regions have a much higher GP (up to 0.6–0.8), matching with Alexa-conjugated α-Bgtx staining (Fig. 2F). However, some well-defined AChR clusters, although showing lower α-Bgtx staining, exhibited a lower GP. These regions probably accounted for the lower mean GP value of AChR clusters. These data are in agreement with early studies by Barrantes and colleagues (51) on the high lipid order of AChR-rich postsynaptic membranes from *Torpedo* fish as studied by Laurdan spectroscopy.

This technique also allowed us to assess the effect of cholesterol depletion on lipid structure in myotubes. In good agreement with the dispersion of AChR clusters or the inhibition of AChR clustering upon MβCD treatment, GP values also decreased significantly to quasi-disordered membrane phases. Because of its limited resolution (183 nm at 800 nm excitation wavelength), the two-photon technique is not capable of visualizing individual rafts with estimated diameters of 30–50 nm. Consequently, we cannot discriminate between the disappearance of AChR rafts from the cell surface and the dispersion of AChR clusters into unresolved small rafts upon cholesterol depletion. These data strengthen our conclusion that AChR-enriched membrane domains are cholesterol-dependent. This is in agreement with other reports (23) but in contrast to raft coalescence in T-cells, in which MβCD treatment diminished membrane order but did not abolish it (39).

Although raft biochemical extraction has raised controversies (52, 53), the demonstration by Gaus et al. (44) that THP-1 macrophages treated with either 0.2% Triton X-100 or sonication yield membranes of similar lipid structure prompted us to biochemically investigate rafts from C2C12 myotubes. We show here that three different biochemical preparations of DRM fractions using either cold Triton X-100 or detergent-free extraction procedures (Figs. 3–6) yielded vesicular light fractions showing remarkable similarity as they are enriched in lipid rafts (cholesterol and ganglioside GM-1), in the raft markers caveolin-3 and flotillin-2, and in AChR. These DRMs also contained syntrophin as well as a small part of rapsyn and MuSK (data not shown), indicating the possibility that the regulation of AChR clustering at synaptic sites by the agrin/MuSK/rapsyn machinery is dependent on rafts. These observations are in agreement with our previous study showing that AChR and rapsyn expressed transiently in COS-7 cells also partitioned in DRMs (22).

Our finding that AChR as well as other synaptic proteins are included within rafts is consistent with the accumulation of cholesterol and GM1 ganglioside in AChR-rich postsynaptic membranes purified from *Torpedo* electric tissue

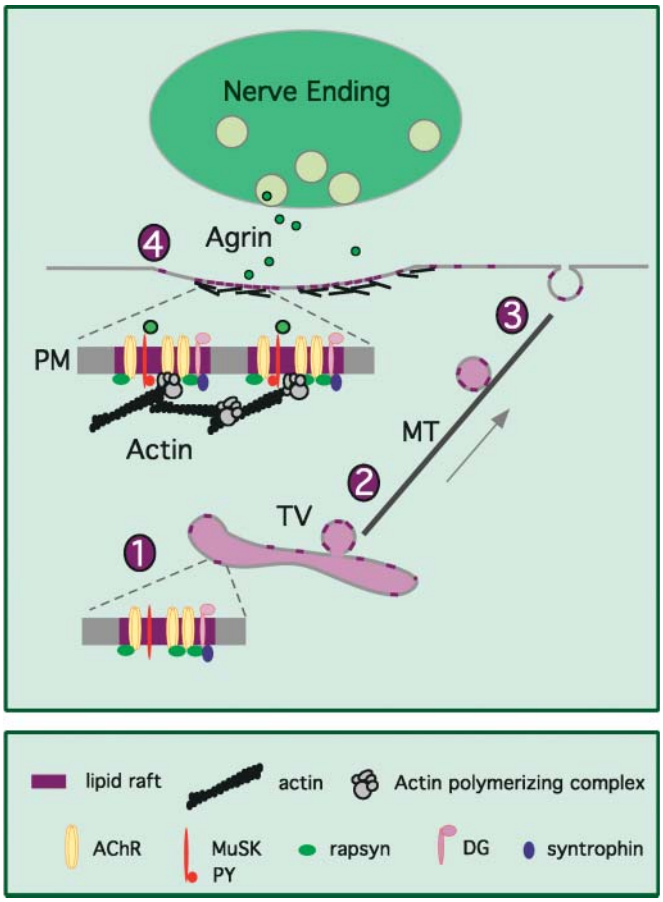

Fig. 9. Model of postsynaptic apparatus formation by agrin-elicited raft coalescence at the neuromuscular junction. Rafts containing various components of the postsynaptic membrane [AChR, muscle-specific kinase (MuSK), rapsyn, syntrophin, etc.] were assembled and sorted in the exocytic compartments (1), transported within vesicles (2), and targeted to the cell surface, via microtubules (3). Tyrosine phosphorylation of MuSK by nerve-secreted agrin would induce actin-driven coalescence of AChR-containing rafts through reorganization of the actin cytoskeleton (4). Alternatively, it is possible that each raft accommodates a different subset of proteins (i.e., AChR, MuSK, or rapsyn). Upon agrin engagement, AChR clustering could occur when many rafts cluster together, forming a large platform where the proteins can meet. DG, dystroglycan; MT, microtubule; PM, postsynaptic membrane; PY, phosphotyrosine; TV, transport vesicle.

(54, 55) and with freeze-fracture data of filipin-treated rat myotubes in which spontaneous AChR clusters appear enriched in cholesterol (56). Cholesterol is also important for AChR function in that it preserves agonist-induced affinity state transitions (57). Moreover, the physical state of the AChR-rich postsynaptic membrane from *Torpedo*, as studied by electron spin resonance (58, 59), showed that the protein-vicinal lipids are immobile relative to the rest of the membrane lipids. Our findings are also in keeping with recent reports showing that several neurotransmitter receptors and ion channels are biochemically located in lipid DRMs and that cholesterol is required for their maintenance at postsynaptic sites or dendritic spines (16).

In a recent publication (23), it was reported that agrin treatment results in an increase in AChR association with lipid rafts. However, this assertion was based on fluorescence experiments, the resolution of which (~200 nm) is far below the estimated size of individual rafts (10–50 nm). As such, it is not possible to deduce from these experiments whether AChRs reside in rafts before clustering. Yet, DRM fractions obtained from untreated myotubes in various extraction conditions (Triton X-100, pH 11, and Ca^{2+}/Mg^{2+} buffer) contained robust amounts of AChR, and we were not able to detect any difference in the distribution patterns of AChRs along the gradients between control and agrin-treated myotubes. These findings suggest that the association of AChRs with DRM is not dependent on agrin. This observation was not surprising because rafts participate in intracellular trafficking and surface targeting of AChR (22). In addition, cells defective in sphingolipid biosynthesis express low amounts of cell surface AChRs (60). Because intracellular trafficking and surface targeting of AChR are not likely to be controlled by agrin, the AChRs delivered to the cell surface are very likely constitutively embedded in rafts. Collectively, these data lead to the notion that agrin activation regulates the coalescence of AChR-containing rafts rather than the recruitment of AChR to rafts.

Considered as platforms for concentrating individual receptors activated by ligand binding, rafts are believed to play important roles at the cell surface through signal transduction (48, 61). Besides the formation of the immunological synapse (62–64), many other signaling pathways, including epidermal growth factor (EGF), glial cell line-derived neurotrophic factor (GNDF), and Ras signaling (48), tyrosine phosphorylation (12), and signaling through phosphatidylinositol-4,5-bisphosphate (65, 66), rely on lipid rafts. In this view, the occurrence of several effectors of the agrin signaling pathway leading to AChR clustering, such as MuSK, rapsyn, and syntrophin, in DRMs is of interest. Accumulating evidence indicates that rafts are too small to engage in membrane function. To trigger signal transduction processes, they usually have to cluster. An attractive hypothesis from this work is that raft coalescence may be an important step of the agrin-induced AChR clustering through the activation of MuSK. Given the small size of individual rafts, it is possible that each raft contains a different subset of proteins (i.e., AChR, MuSK, or rapsyn). Upon agrin engagement, AChR clustering could occur when many rafts cluster together, forming a large platform on which the proteins can meet. Activated platforms could then recruit in a reversible and dynamic manner scaffolding and/or cytoskeletal proteins that promote large raft assembly (67, 68). Along this line, it is worth noting that agrin-induced AChR clustering depends on the actin-driven movement of AChR protein within the sarcolemma (8) and that MuSK activation also triggers actin cytoskeleton reorganization via the activation of Rac/Cdc42 (9, 69, 70). Yet, lipid rafts, as preferred platforms for membrane-linked actin polymerization (68), might serve as nucleation sites for AChR clustering upon MuSK signaling (**Fig. 9**). A raft-regulated AChR clustering process may also be important for synapse specification by keeping raft-borne synaptic proteins in an "off" state to prevent undue AChR clustering outside of synaptic sites.

NOTE ADDED IN PROOF

While this paper was being reviewed, the group of Professor Lin Mei also presented evidence for a role of lipid rafts as signaling platforms for AChR clustering. (Zhu, D., W.C. Xiong, and L. Mei. 2006. *J NeuroSci* **26**:4841–4851).

The authors are indebted to Dr. K. Simons, who gave us the opportunity to collaborate with K.G. in Dresden and for his helpful advice. The authors thank Drs. G. Camus, M. A. Ludosky, S. Marchand, and C. Pato for help during this work as well as Drs. C. Zurzolo and M. C. Marden for advice and critical reading of the manuscript. The authors thank Profs. S. Froehner and J. M. Trowbridge for generous gifts of anti-syntrophin and anti-transferrin receptor antibodies. This work was supported by grants from the Centre National de la Recherche Scientifique, the Association Française Contre les Myopathies, and the Agence Nationale de la Recherche to J.C. K.G. acknowledges support from the Alexander von Humbolt Foundation.

REFERENCES

1. McMahan, U. J. 1990. The agrin hypothesis. *Cold Spring Harb. Symp. Quant. Biol.* **55:** 407–418.
2. Sanes, J. R., and J. W. Lichtman. 2001. Induction, assembly, maturation and maintenance of a postsynaptic apparatus. *Nat. Rev. Neurosci.* **2:** 791–805.
3. Kummer, T. T., T. Misgeld, and J. R. Sanes. 2006. Assembly of the postsynaptic membrane at the vertebrate neuromuscular junction: paradigm lost. *Curr. Opin. Neurobiol.* **16:** 1–9.
4. Glass, D. J., D. C. Bowen, T. N. Stitt, C. Radziejewski, J. Bruno, T. E. Ryan, D. R. Gies, S. Shah, K. Mattsson, S. J. Burden, et al. 1996. Agrin acts via a MuSK receptor complex. *Cell.* **85:** 513–523.
5. Strochlic, L., A. Cartaud, and J. Cartaud. 2005. The synaptic muscle-specific kinase (MuSK) complex: new partners new functions. *Bioessays.* **27:** 1129–1135.
6. Wallace, B. G. 1992. Mechanism of agrin-induced acetylcholine receptor aggregation. *J. Neurobiol.* **23:** 592–604.
7. Hoch, W., J. T. Campanelli, and R. H. Scheller. 1994. Agrin-induced clustering of acetylcholine receptors: a cytoskeletal link. *J. Cell Biol.* **126:** 1–4.
8. Dai, Z., X. Luo, H. Xie, and H. B. Peng. 2000. The actin-driven movement and formation of acetylcholine receptor clusters. *J. Cell Biol.* **150:** 1321–1334.
9. Weston, C., C. Gordon, G. Teressa, E. Hod, X. D. Ren, and J. Prives. 2003. Cooperative regulation by Rac and Rho of agrin-induced acetylcholine receptor clustering in muscle cells. *J. Biol. Chem.* **278:** 6450–6455.

10. Ikonen, E. 2001. Roles of lipid rafts in membrane transport. *Curr. Opin. Cell Biol.* **13:** 470–477.
11. Simons, K., and E. Ikonen. 1997. Functional rafts in cell membranes. *Nature.* **387:** 569–572.
12. Harder, T., and K. Simons. 1999. Clusters of glycolipid and glycosylphosphatidylinositol-anchored proteins in lymphoid cells: accumulation of actin regulated by local tyrosine phosphorylation. *Eur. J. Immunol.* **29:** 556–562.
13. Holowka, D., E. D. Sheets, and B. Baird. 2000. Interactions between Fc (epsilon) RI and lipid raft components are regulated by the actin cytoskeleton. *J. Cell Sci.* **113:** 1009–1019.
14. Harder, T., P. Scheiffele, P. Verkade, and K. Simons. 1998. Lipid domain structure of the plasma membrane revealed by patching of membrane components. *J. Cell Biol.* **141:** 929–942.
15. Friedrichson, T., and T. V. Kurzchalia. 1998. Microdomains of GPI-anchored proteins in living cells revealed by crosslinking. *Nature.* **394:** 802–805.
16. Tsui-Pierchala, B. A., M. Encinas, J. Milbrandt, and E. M. Johnson, Jr. 2002. Lipid rafts in neuronal signaling and function. *Trends Neurosci.* **25:** 412–417.
17. Becher, A., J. H. White, and R. A. McIlhinney. 2001. The gamma-aminobutyric acid receptor B, but not the metabotropic glutamate receptor type-I, associates with lipid rafts in the rat cerebellum. *J. Neurochem.* **79:** 787–795.
18. Brusés, J. L., N. Chauvet, and U. Rutishauser. 2001. Membrane lipid rafts are necessary for the maintenance of the (alpha)7 nicotinic acetylcholine receptor in somatic spines of ciliary neurons. *J. Neurosci.* **21:** 504–512.
19. Hering, H., C. C. Lin, and M. Sheng. 2003. Lipid rafts in the maintenance of synapses, dendritic spines, and surface AMPA receptor stability. *J. Neurosci.* **23:** 3262–3271.
20. Oshikawa, J., Y. Toya, T. Fujita, M. Egawa, J. Kawabe, S. Umemura, and Y. Ishikawa. 2003. Nicotinic acetylcholine receptor α7 regulates cAMP signal within lipid rafts. *Am. J. Physiol. Cell Physiol.* **285:** C567–C574.
21. Martens, J. R., K. O'Connell, and M. Tamkun. 2004. Targeting of ion channels to membrane microdomains: localization of Kv channels to lipid rafts. *Trends Pharmacol. Sci.* **25:** 16–21.
22. Marchand, S., A. Devillers-Thiéry, S. Pons, J. P. Changeux, and J. Cartaud. 2002. Rapsyn escorts the nicotinic acetylcholine receptor along the exocytic pathway via association with lipid rafts. *J. Neurosci.* **20:** 8891–8901.
23. Campagna, J. A., and J. Fallon. 2006. Lipid rafts are involved in C95 (4,8) agrin fragment-induced acetylcholine receptor clustering. *Neuroscience.* **138:** 123–132.
24. Edidin, M. 2003. The state of lipid rafts: from model membranes to cells. *Annu. Rev. Biophys. Biomol. Struct.* **32:** 257–283.
25. Munro, S. 2003. Lipid rafts: elusive or illusive? *Cell.* **115:** 377–388.
26. Gaus, K., T. Zech, and T. Harder. 2006. Visualizing membrane macrodomains by Laurdan 2-photon microscopy. *Mol. Membr. Biol.* **23:** 41–48.
27. Froehner, S. C., A. A. Murnane, M. Tobler, H. B. Peng, and R. Sealock. 1987. A postsynaptic Mr 58,000 (58K) protein concentrated at acetylcholine receptor-rich sites in Torpedo electroplaques and skeletal muscle. *J. Cell Biol.* **104:** 1633–1646.
28. Peng, H. B., and S. C. Froehner. 1985. Association of the postsynaptic 43K protein with newly formed acetylcholine receptor clusters in cultured muscle cells. *J. Cell Biol.* **100:** 1698–1705.
29. Brown, D. A., and J. K. Rose. 1992. Sorting of GPI-anchored proteins to glycolipid-enriched membrane subdomains during transport to the apical cell surface. *Cell.* **68:** 533–544.
30. Song, K. S., S. Li, T. Okamoto, L. A. Quilliam, M. Sargiacomo, and M. P. Lisanti. 1996. Co-purification and direct interaction of Ras with caveolin, an integral membrane protein of caveolae microdomains. Detergent-free purification of caveolae microdomains. *J. Biol. Chem.* **271:** 9690–9697.
31. Macdonald, J. L., and L. J. Pike. 2005. A simplified method for the preparation of detergent-free lipid rafts. *J. Lipid Res.* **46:** 1061–1067.
32. Laemmli, U. K. 1970. Cleavage of structural proteins during the assembly of the head of bacteriophage T4. *Nature.* **227:** 680–685.
33. Gaus, K., E. Gratton, E. P. Kable, A. S. Jones, I. Gelissen, L. Kritharides, and W. Jessup. 2003. Visualizing lipid structure and raft domains in living cells with two-photon microscopy. *Proc. Natl. Acad. Sci. USA.* **100:** 15554–15559.
34. Green, W. N., and C. P. Wanamaker. 1998. Formation of the nicotinic acetylcholine receptor binding sites. *J. Neurosci.* **15:** 5555–5564.
35. Kahl, J., and J. T. Campanelli. 2003. A role for the juxtamembrane domain of beta-dystroglycan in agrin-induced acetylcholine receptor clustering. *J. Neurosci.* **23:** 392–402.
36. Scheiffele, P., M. G. Roth, and K. Simons. 1997. Interaction of influenza virus haemagglutinin with sphingolipid-cholesterol membrane domains via its transmembrane domain. *EMBO J.* **16:** 5501–5508.
37. Olson, E. N., L. Glaser, and J. P. Merlie. 1984. α and β subunits of the nicotinic acetylcholine receptor contain covalently bound lipid. *J. Biol. Chem.* **259:** 5364–5367.
38. Pediconi, M. F., C. E. Gallegos, E. B. De Los Santos, and F. J. Barrantes. 2004. Metabolic cholesterol depletion hinders cell-surface trafficking of the nicotinic acetylcholine receptor. *Neuroscience.* **128:** 239–249.
39. Gaus, K., E. Chklovskaia, B. Fazekas de St. Groth, W. Jessup, and T. Harder. 2005. Condensation of the plasma membrane at the site of T-lymphocyte activation. *J. Cell Biol.* **171:** 121–131.
40. Song, K. S., P. E. Scherer, Z. L. Tang, T. Okamoto, S. Li, M. Chafel, C. Chu, S. Kohtz, and M. P. Lisanti. 1996. Expression of caveolin-3 in skeletal, cardiac, and smooth muscle cells. Caveolin-3 is a component of the sarcolemma and co-fractionates with dystrophin and dystrophin-associated glycoproteins. *J. Biol. Chem.* **271:** 15160–15165.
41. Volonté, D., F. Galbiati, S. Li, K. Nishiyama, T. Okamoto, and M. P. Lisanti. 1999. Flotillins/cavatellins are differentially expressed in cells and tissues and form a hetero-oligomeric complex with caveolins *in vivo.* Characterization and epitope-mapping of a novel flotillin-1 monoclonal antibody probe. *J. Biol. Chem.* **274:** 12702–12709.
42. Bloch, R. J., W. G. Resneck, A. O'Neill, J. Stron, and D. W. Pumplin. 1991. Cytoplasmic components of acetylcholine receptor clusters of cultured rat myotubes: the 58-kD protein. *J. Cell Biol.* **115:** 435–446.
43. Schuck, S., M. Honsho, K. Ekroos, A. Shevchenko, and K. Simons. 2003. Resistance of cell membranes to different detergents. *Proc. Natl. Acad. Sci. USA.* **100:** 5795–5800.
44. Gaus, K., M. Rodriguez, K. R. Ruberu, I. Gelissen, T. M. Sloane, L. Kritharides, and W. Jessup. 2005. Domain specific lipid distribution in macrophage plasma membrane. *J. Lipid Res.* **46:** 1526–1538.
45. Konno, D., J. A. Ko, S. Usui, K. Hori, H. Maruoka, M. Inui, T. Fujikado, Y. Tano, T. Suzuki, K. Tohyama, et al. 2002. The post-synaptic density and dendritic raft localization of PSD-Zip70, which contains an N-myristoylation sequence and leucine-zipper motifs. *J. Cell Sci.* **115:** 4695–4706.
46. Pralle, A., P. Keller, E. L. Florin, K. Simons, and J. K. H. Hörber. 2000. Sphingolipid-cholesterol rafts diffuse as small entities in the plasma membrane of mammalian cells. *J. Cell Biol.* **148:** 997–1007.
47. Galbiati, F., B. Razani, and M. P. Lisanti. 2001. Emerging themes in lipid rafts and caveolae. *Cell.* **106:** 403–411.
48. Simons, K., and D. Toomre. 2000. Lipid rafts and signal transduction. *Nat. Rev. Mol. Cell Biol.* **1:** 31–39.
49. Schuck, S., and K. Simons. 2004. Polarized sorting in epithelial cells: raft clustering and the biogenesis of the apical membrane. *J. Cell Sci.* **117:** 5955–5964.
50. Kindzelskii, A. L., R. G. Sitrin, and H. R. Petty. 2004. Cutting edge. Optical microspectrophotometry supports the existence of gel phase lipid rafts at the lamellipodium of neutrophils: apparent role in calcium signaling. *J. Immunol.* **172:** 4681–4685.
51. Antollini, S. S., M. A. Soto, I. C. Bonini de Romanelli, C. Gutierrez-Merino, P. Sotomayor, and F. J. Barrantes. 1996. Physical state of bulk and protein-associated lipid in nicotinic acetylcholine receptor-rich membrane studied by Laurdan generalized polarization and fluorescence energy transfer. *Biophys. J.* **70:** 1275–1284.
52. Chamberlain, L. H. 2004. Detergents as tools for the purification and classification of lipid rafts. *FEBS Lett.* **559:** 1–5.
53. Lichtenberg, D., F. M. Goñi, and H. Heerklotz. 2005. Detergent-resistant membranes should not be identified with membrane rafts. *Trends Biochem. Sci.* **30:** 430–436.
54. Popot, J. L., R. A. Demel, A. Sobel, L. L. Van Deenen, and J. P. Changeux. 1978. Interaction of the acetylcholine (nicotinic) receptor protein from *Torpedo marmorata* electric organ with monolayers of pure lipids. *Eur. J. Biochem.* **85:** 27–42.
55. Marcheselli, V., J. L. Daniotti, A. C. Vidal, H. Maccioni, D. Marsh, and F. J. Barrantes. 1993. Gangliosides in acetylcholine receptor-rich membranes from *Torpedo marmorata* and *Discopyge tschudii*. *Neurochem. Res.* **18:** 599–603.
56. Pumplin, D. W., and R. J. Bloch. 1983. Lipid domains of acetylcholine receptor clusters detected with saponin and filipin. *J. Cell Biol.* **97:** 1043–1054.
57. Barrantes, F. J. 2004. Structural basis for lipid modulation of nicotinic acetylcholine receptor function. *Brain Res. Rev.* **47:** 71–95.

58. Marsh, D., and F. J. Barrantes. 1978. Immobilized lipid in acetylcholine receptor-rich membranes from *Torpedo marmorata*. *Proc. Natl. Acad. Sci. USA.* **75:** 4329–4333.
59. Rousselet, A., P. F. Devaux, and K. W. Wirtz. 1979. Free fatty acids and esters can be immobilized by receptor rich membranes from *Torpedo marmorata* but not phospholipid acyl chains. *Biochem. Biophys. Res. Commun.* **90:** 871–877.
60. Roccamo, A. M., M. F. Pediconi, E. Aztiria, L. Zanello, A. Wolstenholme, and F. J. Barrantes. 1999. Cells defective in sphingolipids biosynthesis express low amounts of muscle nicotinic acetylcholine receptor. *Eur. J. Neurosci.* **11:** 1615–1623.
61. Pierce, S. 2002. Lipid rafts and B-cell activation. *Nat. Rev. Immunol.* **2:** 96–105.
62. Sheets, E. D., D. Holowka, and B. Baird. 1999. Membrane organization in immunoglobulin E receptor signaling. *Curr. Opin. Chem. Biol.* **3:** 95–99.
63. Janes, P. W., S. C. Ley, A. I. Magee, and P. S. Kabouridis. 2000. The role of lipid rafts in T cell antigen receptor (TCR) signalling. *Semin. Immunol.* **12:** 23–34.
64. Langlet, C., A. M. Bernard, P. Drevot, and H. T. He. 2000. Membrane rafts and signaling by the multichain immune recognition receptors. *Curr. Opin. Immunol.* **12:** 250–255.
65. Fujimoto, T., S. Nakade, A. Miyawaki, K. Mikoshiba, and K. Ogawa. 1992. Localization of inositol 1,4,5-trisphosphate receptor-like protein in plasmalemmal caveolae. *J. Cell Biol.* **119:** 1507–1515.
66. Pike, L. J., and L. Casey. 1996. Localization and turnover of phosphatidylinositol 4,5-bisphosphate in caveolin-enriched membrane domains. *J. Biol. Chem.* **271:** 26453–26456.
67. Pike, L. J., and J. M. Miller. 1998. Cholesterol depletion delocalizes phosphatidylinositol bisphosphate and inhibits hormone-stimulated phosphatidylinositol turnover. *J. Biol. Chem.* **273:** 22298–22304.
68. Rozelle, A. L., L. M. Machesky, M. Yamamoto, M. H. E. Driessens, R. H. Insall, M. G. Roth, K. Luby-Phelps, G. Marriott, A. Hall, and H. L. Yin. 2000. Phosphatidylinositol 4,5-bisphosphate induces actin-based movement of raft-enriched vesicles through WASP-Arp2/3. *Curr. Biol.* **10:** 311–320.
69. Weston, C., B. Yee, E. Hod, and J. Prives. 2000. Agrin-induced acetylcholine receptor clustering is mediated by small guanosine triphosphatases Rac and Cdc42. *J. Cell Biol.* **150:** 205–212.
70. Luo, Z. G., Q. Wang, J. Z. Zhou, J. Wang, Z. Luo, M. Liu, X. He, A. Wynshaw-Boris, W. C. Xiong, B. Lu, et al. 2002. Regulation of AChR clustering by Dishevelled interacting with MuSK and PAK1. *Neuron.* **35:** 489–505.